Apparent heat capacity method to describe the thermal performances of a latent thermal storage system during discharge period

A. El Ouali, Y. Khattari, B. Lamrani, T. El Rhafiki, Y. Zeraouli, Tarik Kousksou

Version of Record: https://www.sciencedirect.com/science/article/pii/S2352152X22009665
Manuscript_87f461d1cd44d3bcffdf32c66a9c4a5a

Apparent heat capacity method to describe the thermal performances of a latent thermal storage system during discharge period

A. El Ouali [(a)], Y. Khattari[(b)], B. Lamrani [(c)], T. El Rhafiki[(d)], Y. Zeraouli[(b)], T. Kousksou[(b)]

[(a)] Mohammed V University in Rabat, Materials, Energy and Acoustics TEAM (MEAT), avenue Prince Héritier, B.P:227 salé Médina, Morocco.

[(b)] Université de Pau et des Pays de l'Adour, E2S UPPA, SIAME, Pau, France

[(c)] Mohammed V University in Rabat, Faculty of Sciences, MANAPSE Laboratory, 1014 RP, Rabat, Morocco.

[(d)]Engineering Sciences Laboratory, Polydisciplinary Faculty of Taza, Sidi Mohamed Ben-Abdellah University Fez, Morocco

Abstract:

In this work, a novel detailed dynamic model for latent cold thermal storage unit containing water as phase change material (PCM) is presented. The proposed dynamic model is based on transient energy balances for both PCM capsules and heat transfer fluid (HTF). The apparent heat capacity approach is used to model phase transition processes in PCM, where the PCM heat capacity is given as a temperature-dependent function. This method can be simply integrated into a variety of software to assess the energy efficiency of latent storage. The dynamic model of the PCM storage unit is validated using measured results from the literature and it is used to investigate the influence of multiple parameters on the storage thermal performance. The obtained result show that the PCM melting process varies in both axial direction and radial direction in the storage unit. It was also observed that the higher the height of the tank, the longer the discharge period. Increasing the diameter of capsules from 47 mm to 77 mm leads to increase the discharging period by about 30 %. In addition, varying the storage tank initial temperature between -8 °C to – 4 °C does not have a significant effect of on the discharging time. Finally, it was recommended that for improving the storage performance and minimizing water pumper energy consumption, a compromise between the HTF flow rate and the capsule diameter must be determined.

Keywords: Latent storage system; cold storage; PCM; Apparent heat capacity; Packed bed; Heat transfer.

Nomenclature

A_f	specific surface of the capsule (m-1)
cp	specific heat ($J.kg^{-1}.K^{-1}$)
d	diameter (m)
H	height tank (m)
Lf	latent heat ($J.kg^{-1}$)
Pr	Prandtl number
q_v	flow rate ($m^3.h^{-1}$)
r	rayon (m)
Ra	Rayleigh number
Re	Reynolds number
t	time (s)
T	temperature (°C)
u	velocity ($m.s^{-1}$)
U_f	convective transfer coefficient ($W.m^{-2}.K^{-1}$)
x	position along the direction of the tank (m)

Greek letters

β	liquid fraction
ρ	density ($kg.m^{-3}$)
μ	dynamic viscosity ($Pa.s^{-1}$)
λ	thermal conductivity ($W.m^{-1}.K^{-1}$)
ε	porosity

Subscripts

App	apparent
HTF	heat transfer fluid
f	fluid
l	liquid
m	melting
PCM	phase change material
s	solid

1. Introduction

Thermal storage systems using phase change materials are presently used in several industrial applications [1] such as waste heat recovery [2], industrial cold [3-4], HVAC [5], district heating [6-7], thermal management of electronic devices and batteries [8-9]. Such systems are considered indispensable to support the energy transition and manage the intermittency of renewable energies [10-12].Thermal storage systems using phase change materials (PCMs) are advantageous as they allow thermal energy to be stored close to their melting temperature in a specified storage volume [13]. When demand for thermal energy is lower than production, the latent thermal storage system stores the unused thermal energy. On the other hand, during periods of peak consumption, the thermal storage system releases the accumulated thermal energy [14-15].

Usually, PCM is enclosed in capsules, which can be spherical, cylindrical or rectangular [16-17]. Other geometries are under development such as biomimetic red blood cell (RBC) shaped capsules for thermal storage of latent heat. The RBC shape offers a considerably higher heat transfer rate than other shapes [11-12]. However, research is underway to characterize the heat transfer between these capsules and the heat transfer fluid in the storage tanks [11-12].

Spherical capsules are widely used for industrial applications [18-20]. Using this geometry, the heat transfer surface between the heat transfer fluid (HTF) and the PCM can be enhanced. Several studies have been carried out on the numerical analysis and physical modeling of the transition process inside a tank filled with PCMs enclosed in spherical capsules [21]. The thermal performance of a latent storage system has been evaluated using different physical models such as the homogeneous model [22-23], the Schumann model [24-26], the continuous solid phase model [27-32] and the concentric diffusion model [33-38]. All of these models consider that the packed bed system acts as a porous medium [21]. The homogeneous model is rarely used as the assumption of a single local temperature for both solid and liquid media is only valid if the PCM capsule have a conductivity close to that of the fluid or when they have a small diameter [39]. Schumann's model ignores the thermal conduction inside the particle. However, when the thermal conductivity of the PCM is low (which is the majority of cases) or when the particle size is high, then the internal thermal resistance cannot be neglected [40]. The continuous solid phase model considers PCM capsules as a continuous medium and not as a medium composed of independent spherical capsules. Therefore, the internal thermal conduction in the particle is not taken into account. On the other hand, the conduction in the axial (one-dimensional model) direction is considered [31-32]. The

concentric diffusion model is a heterogeneous two-phase model that has the characteristic of considering the thermal conduction inside the PCM capsules. As the shape of the capsules is spherical, the thermal conduction is radial [41-42]. This model is indeed the only one taking into account the radial heat conduction within the PCM, even if it increases considerably the computation time. The thermal radial conduction is important especially when the flow rate is low [43-47]. As an example, Peng et al. [46] studied the comportment of a PCM capsules inside the tank. The transition process within the PCM is analysed using the enthalpic method. The results obtained are validated with the experimental results of Izquierdo-Barrientos et al. [47]. The authors [47] indicate that decreasing the size of the PCM capsule or the fluid inlet velocity, or increasing the bed height increase the thermal efficiency of the system. Tafone et al. [48] adopted the concentric diffusion model to investigate the packed bed contained spherical PCM capsules for liquid air energy storage system. The apparent heat capacity approach was adopted to address the phase transition inside the capsule. The same model was also employed by Li et al. [49-50] to address the thermal performance of a latent storage system containing PCM confined in spherical capsules. The authors [49-50] indicate that the performance of the system can be improved by the HTF inlet temperature and the mass flow rate of the latter. They also showed that a smaller capsule diameter results in better system performance and that an increase in the size of the capsules leads to an increase in the melting process time. It is important to note that in most of the studies using the concentric diffusion model, authors present only the evolution of the HTF temperature in the packed bed. To the best of the authors' knowledge, the evolution of the temperature within the PCM as a function of the spherical capsule radius during the discharge period has not been reported in any of the previously mentioned papers.

The expression of heat capacity and enthalpy of PCM as a function of temperature during the phase transition process is essential for correct mathematical modelling of heat transfer inside the spherical capsules. However, when the physical model is derived from the apparent capacity approach, the heat transfer inside the PCM can be described by a single energy equation. This simplifies the mathematical resolution of the differential equations that describe the flow and heat transfer in the latent storage tanks. Our original contribution in this work lies in the following main points:

- A physical model based on the apparent heat capacity approach has been developed to investigate the thermal performances of the packed bed. The physical model was then validated based on experimental results from the literature.

- We propose a complementary analysis of the phase transition inside the capsules at different positions in the tank.
- The influence of different parameters on the thermal performance of the tank has also been highlighted.

2. Physical model

Fig.1 illustrates the Latent Storage System used in this study. It consists of a cylindrical tank with a height L and a diameter d_t. The tank contains a PCM confined in spherical capsules placed randomly with a porosity $\mathcal{E}$. The capsules have a diameter d_{pcm} and are made of high polyethylene density. During the charging/discharging process, the heat transfer fluid (HTF) moves in at a constant temperature from the bottom of the tank to give up/accumulate heat by convective transfer. HTF used in our study will be water. The charging/discharging process is considered complete when the temperature becomes uniform on the whole system. The main parameters of our storage system are summarised in **Table 1**.

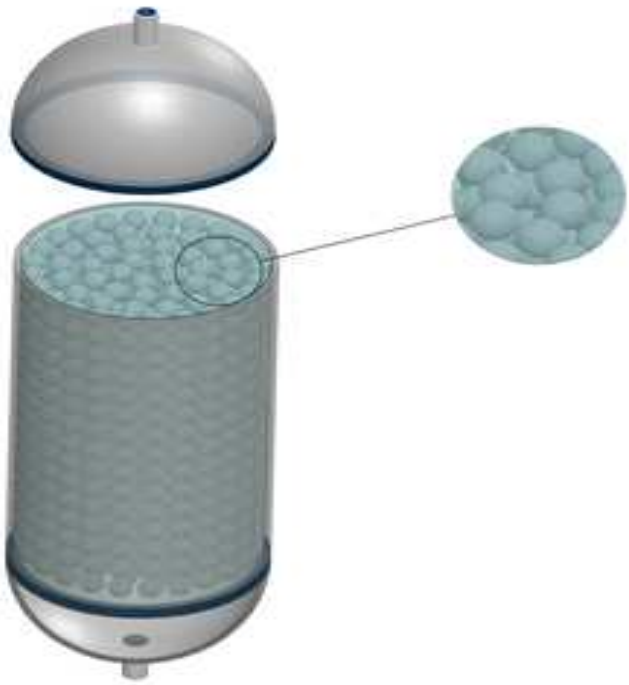

Fig.1: Latent storage system

Table 1: Main parameters of the storage tank

Parameters	Valuer
Tank height (H) [m]	*1, 1.42, 2*
Tank diameter (d_t) [m]	*0.95*
Capsule diameter (d_{pcm}) [mm]	*47, 67, 77*
Porosity (ε)	*0.4*
HTF flow rate (q_v) [$m^3.h^{-1}$]	*1, 1.5, 2.3, 2.6, 3*
HTF initial temperature [°C]	*-4, -6, -8*

Before describing the physical model, it is fundamental to specify the main assumptions:

- The tank is assumed to be perfectly insulated.
- The flow of the HTF is monodirectional from the bottom to the top.
- Heat conduction in the spherical capsules occurs radially (i.e. constrained melting).
- The spherical capsules are considered as an isotropic porous medium.
- The packed bed is divided it into several layers in the axial direction. All the spheres of the same layer are assumed to act similarly and each layer can be modelled and discretized using a single sphere.

The system of energy conservation equations consists of two coupled expressions: one equation for the HTF and another for PCM. By considering the previously mentioned assumptions, the equations of the model are the following:

- ***For HTF***:

$$\rho_f c_f \varepsilon \frac{\partial T_f}{\partial t} + \varepsilon \rho_f c_f u_f \frac{\partial T_f\left(x,t\right)}{\partial x} = \varepsilon \lambda_f \frac{\partial^2 T_f\left(x,t\right)}{\partial x^2} + U_f A_f \left(T_{pcm}(r=\frac{d}{2}) - T_f\left(x,t\right) \right)$$

(1)

- ***For PCM***:

$$\rho_{pcm} c_{pcm} \frac{\partial T_{pcm}(r,t)}{\partial t} = \frac{1}{r^2} \frac{\partial}{\partial r} \left(r^2 \lambda_{pcm} \frac{\partial T_{pcm}(r,t)}{\partial r} \right)$$

(2)

where, T_f and T_{pcm} indicate the HTF and PCM temperature respectively, u_f is the HTF velocity, c_f is the specific heat capacity of the HTF, c_{pcm} is the apparent heat capacity of the PCM, ρ_f is the HTF density, ρ_{pcm} is the PCM density, λ_f is the thermal conductivity of HTF, λ_{pcm} is the thermal conductivity of PCM and ε is the porosity of the packed bed. The coefficient A_f is the specific surface of the capsule per unit volume and is expressed as follows:

$$A_f = \frac{6(1-\varepsilon)}{d_{capsule}} \quad \textbf{(3)}$$

The convective transfer coefficient U_f between the HTF and the capsules is defined by [51]:

$$U_f = \frac{\lambda_f}{d}\left[3.22\,\mathrm{Re}^{1/3}\,\mathrm{Pr}^{1/3} + 0.117\,\mathrm{Re}^{0.8}\,\mathrm{Pr}^{0.8}\right] \quad \textbf{(4)}$$

The Reynolds and Prandtl numbers can be written as follows:

$$\mathrm{Re} = \frac{\rho_f d_{capsule} \varepsilon u_f}{\mu_f} \quad \textbf{(5)}$$

$$\mathrm{Pr} = \frac{c_{p,f}\mu_f}{\lambda_f} \quad \textbf{(6)}$$

When the physical model is derived from the apparent capacity approach, the heat transfer inside the PCM can be described by a single energy equation. This makes it easier to solve the differential equations that describe the flow and heat transfer in storage tanks properly. In our case, the apparent heat capacity and the thermal conductivity of the PCM is calculated by using the following expressions [52][9]:

$$c_{pcm} = \beta c_{pcm,l} + (1-\beta) c_{pcm,s} + L_f \frac{\frac{2\gamma}{\Delta T}}{\pi\left[\left(\left(T-T_m\right)\left(\frac{2\gamma}{\Delta T}\right)\right)^2 + 1\right]} \quad \textbf{(7)}$$

where $c_{pcm,l}$ and $c_{pcm,s}$ are the specific heat capacity of PCM in solid and liquid states, ΔT is the width of the melting phase temperature, and T_m is the melting temperature of the PCM. β is the liquid fraction which can be calculated by the following expression [52]:

$$\beta = \frac{1}{2}\left[\tanh\left[\frac{2\gamma\left(T - T_m\right)}{\Delta T}\right] + 1\right] \quad \textbf{(8)}$$

Furthermore, our physical model also needs to consider the variation of the PCM thermophysical properties during phase transition:

$$\rho_{pcm} = \beta\rho_{pcm,l} + \left(1-\beta\right)\rho_{pcm,s}$$

$$\textbf{(9)}\ \lambda_{pcm} = \beta\lambda_{pcm,l} + \left(1-\beta\right)\lambda_{pcm,s}^{eff}$$

(10-a)

where $\lambda_{pcm,s}$ and $\lambda_{pcm,l}^{eff}$ are thermal conductivities of PCMs in solid and liquid states and $\rho_{pcm,s}$ and $\rho_{pcm,l}$ are densities of PCM in solid and liquid states.

During constrained melting, heat conduction acts only at the initial stage of the melting process. This leads to a nearly concentric melting of the PCM inside the spherical capsule [53]. During the melting process, an oval shape emerges in the upper part of the solid PCM, but the profile of the lower part remains relatively unchanged. The oval shape is caused by natural convection as the liquid layer increases [54]. Natural convection occurs because the hot liquid in the PCM rises while the cooler liquid flows down to replace the hotter fluid. This creates an unsteady fluid flow inside the capsule, known as buoyancy-driven convection. The top part of the solid PCM melts faster than the bottom part. Natural convection also occurs in the lower half of the spherical capsule, resulting in the wavy profile of the lower part of the solid PCM [55]. In our physical model, the correlation suggested by Lacroix [56] is chosen to evaluate the effective thermal conductivity by including the natural convection occurring during the fusion process:

$$\lambda_{eff,pcm}^{l} = a.Ra^{b}.\lambda_{pcm}^{l} \quad \textbf{(10-b)}$$

where, a and b are constants and equal to 0.05 and 0.5, respectively. The Rayleigh number Ra is computed using the following expression:

$$Ra = \left(\beta \ g \left(\rho c \right)_{pcm}^{l} d^{3} \left| T_f - T_m \right| / \left(\mu_{pcm}^{l} \lambda_{pcm}^{l} \right) \right) \quad \textbf{(10-c)}$$

where, g is the gravitational acceleration, β is the PCM thermal expansion coefficient and μ_{pcm}^{l} is the dynamic viscosity of the liquid PCM.

The initial and boundary conditions of the latent storage system are:

$$t = 0; \forall x; \forall r \qquad T_f \left(x, t = 0 \right) = T_{pcm} \left(r, t = 0 \right) = T_{ini}$$

(11)

$$x = 0; t > 0 \qquad T_f \left(x, t \right) = T_{f,inlet}$$

(12)

$$x = L; t > 0 \qquad \frac{\partial T_f \left(x = L, t \right)}{\partial x} = 0$$

(13)

$$r = 0; t > 0 \qquad \frac{\partial T_{pcm} (\mathrm{r} = 0, t)}{\partial r} = 0$$

(14)

At the capsule wall:

$$r = r_0 \, ; t > 0 \qquad -\lambda_{pcm} \frac{\partial T_{pcm} (\mathrm{r} = r_0 \, , t)}{\partial r} = U_f \left(T_{pcm, r = r_0} - T_f \right)$$

(14)

3. Numerical method

The fully implicit finite volume method was implemented to solve the system of energy equations. The first-order upwind scheme was used to address the convection terms, and the diffusion terms are discretized employing the second-order central differential scheme. Accordingly, the resulting energy equation system can be written as follows:

- ***HTF***

$$a_{f,P}T_{f,P} = a_{f,W}T_{f,W} + a_{f,E}T_{f,E} + a^{0}_{f,P}T^{0}_{f,P} + b_f \quad \textbf{(15)}$$

With :

$$a_{f,P} = a_{f,W} + a_{f,E} + U_f A_f \Delta x$$

(16)

$$a_{f,\mathrm{W}} = \frac{\varepsilon\lambda_f}{\Delta x} + \varepsilon\rho_f c_f \frac{u}{2};\ a_{f,\mathrm{E}} = \frac{\varepsilon\lambda_f}{\Delta x} - \varepsilon\rho_f c_f \frac{u_f}{2};\ b_f = U_f A_f T_{pcm}\left(\mathrm{r}_0, t\right)$$

(17)

- ***PCM***

$$a_{\mathrm{pcm},P}T_{\mathrm{pcm},P} = a_{\mathrm{pcm},W}T_{\mathrm{pcm},W} + a_{\mathrm{pcm},E}T_{\mathrm{pcm},E} + a^{0}_{\mathrm{pcm},P}T^{0}_{\mathrm{pcm},P}$$

(18)

With :

$$a_{\mathrm{pcm},P} = a^{0}_{pcm,P} + a_{pcm,\mathrm{W}} + a_{pcm,\mathrm{E}}$$

(19)

$$a^{0}_{pcm} = \rho_{pcm} c_{pcm} \left(\frac{r_E^2 - r_W^2}{3\Delta t} \right);\ a_{pcm,W} = \frac{r_W^2 \lambda_{pcm,W}}{\Delta r};\ a_{pcm,\mathrm{E}} = \frac{r_E^2 \lambda_{pcm,\mathrm{E}}}{\Delta r} \quad \textbf{(20)}$$

where *E* and *W* are the East and West of each control volume. r_E and r_W refer to the local radius of the P control volume faces. In this work, equations **15** and **18** were solved iteratively using a tridiagonal matrix algorithm (TDMA) method [57]. The computational process was carried out using Fortan 90. The iteration that was specified in each time interval was considered convergent when the maximum relative residual of T_f *and* T_{pcm} was less than 10^{-4}.

4. Model validation

Before reporting, the results related to our study, it is necessary to verify our numerical model. For this purpose, experimental results presented by Bedecarrats et al. [58] are relied

on. In their study, Bedecarrats et al. [58] presented experimental results during the fusion phase inside a tank charged with a spherical capsule enclosing water as a PCM (see **Table 2**). The latent storage system is a cylinder with a height of 1.42 m and a diameter of 0.95 m. Polyurethane foam was employed to insulate the tank thermally. The capsules are filled with water as PCM and are 77 mm in diameter. At the initial instant, the tank temperature (HTF (glycol water) and PCM) is equal to -6°C. The PCM, in that case, is in the solid state (ice). During the discharge period, the HTF flows in the storage tank from the top to the bottom. The HTF temperature at the entry of the tank increases progressively during the first hours to reach a final temperature (T_s) of about +6°C.

Table 2: Main properties of water

Density ($kg.m^{-3}$) Solid Liquid	 917 1000
Latent heat ($kJ.kg^{-1}$)	333
Melting temperature (°C)	0
Specific heat capacity ($J.kg^{-1}.°K^{-1}$) Solid Liquid	 2040 4220
Thermal conductivity ($W.m^{-1}.K^{-1}$) Solid Liquid	 2.25 0.6

It's worth noting that the phase transition happens outside of the melting temperature during the charge phase (crystallisation). A delay in the crystallization is often due to the presence of the supercooling phenomenon [59-60]. This phenomenon can be simulated using the nucleation laws [59-60]. In the following, numerical simulations will be carried out during the discharge period (i.e. melting process), based on a tank initially considered at the initial temperature T_i . We assumed that the moment when the HTF temperature at the outlet of the

tank reaches that of the inlet corresponds to the end of the discharge process. Several simulations were performed to illustrate the effect of HTF flow rate, capsules diameter, tank height and the initial temperature of the system.

The comparison between the experiment and numerical model is presented in **Fig.2-a** through the variation of the HTF temperature at the exit of the tank versus time for various flow rates. The numerical results seem to be in close accord with the experimental ones, thus allowing the validation of the model (see **Fig.2-a**). As shown in this plot, the higher the HTF flow rate, the lower the discharge time. As the HTF flow rate increases, the heat transfer coefficient between capsules and HTF increases. For the three HTF flow rates considered, all the thermal latent energy of the PCM has been recovered by the HTF.

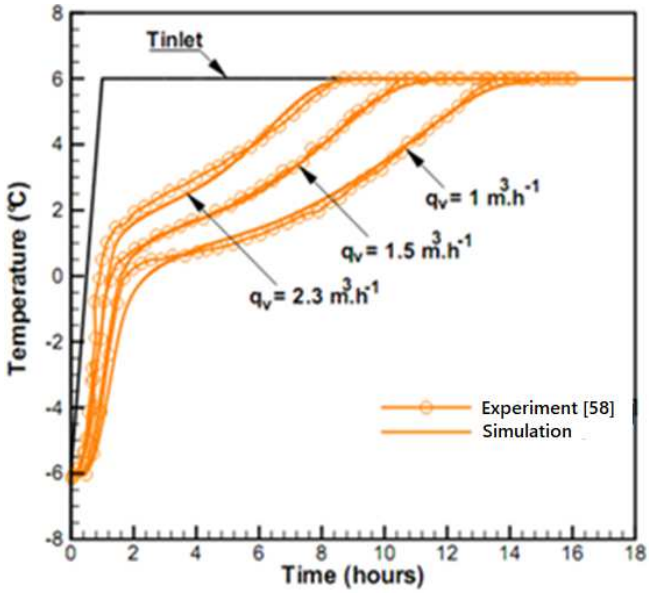

Fig.2-a: HTF temperature versus time at the exit of the system for various flow rates.

We consider that a significant increase in the flow rate does not necessarily imply a significant effect on the discharge time. Moreover, this leads us to think that there would be a limit value of the HTF flow rate, beyond which the discharge time would not decrease anymore (see **Fig.2-b**).

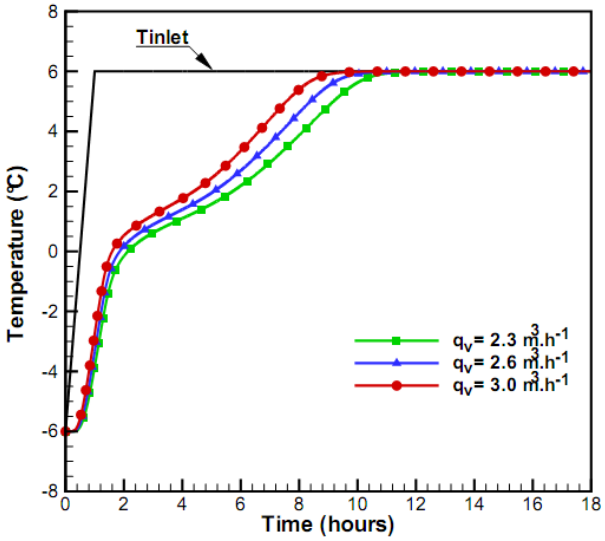

Fig.2-b: Effect of the HTF flow rate on the discharge duration

It is important to note that Bedecarrats et al. **[59]** and Kousksou et al. **[60]** have also developed a physical model of this system by taking into account the thermal conduction in the PCM. In their paper, the authors report only the HTF temperature evolution inside the packed bed. The PCM temperature variation along the radius of the capsules and across the storage tank has not been mentioned in their work **[59-60]**.

In **Fig.3**, we presented the evolution of the HTF temperature between the inlet and the outlet of the tank. The capsule diameter is 77 mm and the tank height is 1.42 m. This graph shows clearly that the fluid flow in the tank is stratified and piston flow.

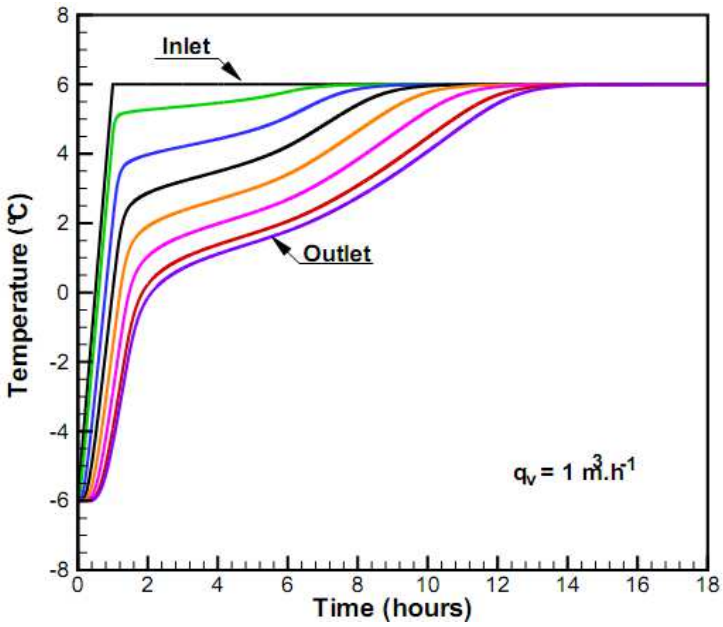

Fig.3: HTF temperature versus time for various positions inside the tank

5. Results and discussion

The physical model is now used to determine the PCM temperature evolution within the capsules for different locations in the tank (see **Fig.4**). We notice that the time of PCM melting in capsules located at the inlet of the tank is shorter than that of capsules situated at the outlet of the tank. Similar tendancies have been found by other authors for a storage tank using other phase change materials [49-50]. The curves also indicate that the temperature gradient in the capsules decreases between the inlet and outlet of the tank. Such results can be attributed to the higher HTF temperature level at the tank inlet compared to that at the tank outlet. This helps to enhance the heat transfer between the HTF and the PCM and accelerate the melting process inside the capsules. In fact, the phase change process leads to a sudden variation and discontinuities in thermodynamic properties. This renders the mathematical modeling of the phase transition more challenging **[61-62]**. However, the results obtained indicate that the phase change of the PCM (i.e. ice) is not occurring at 0°C, but over a range of temperature. This is due to the apparent capacity approach, which was employed in the present work to simulate the melting process in the capsules.

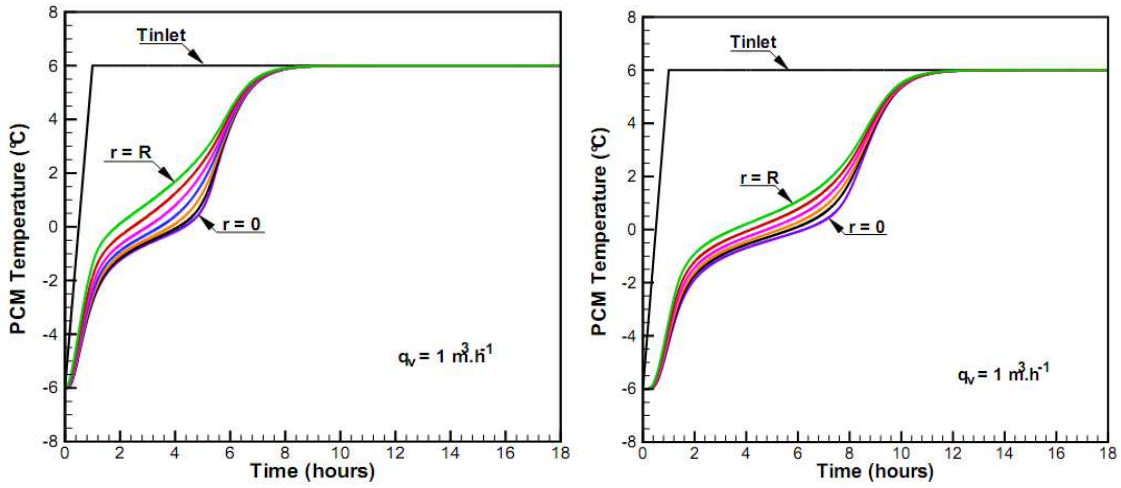

(a) Tank inlet (b) Middle of the tank

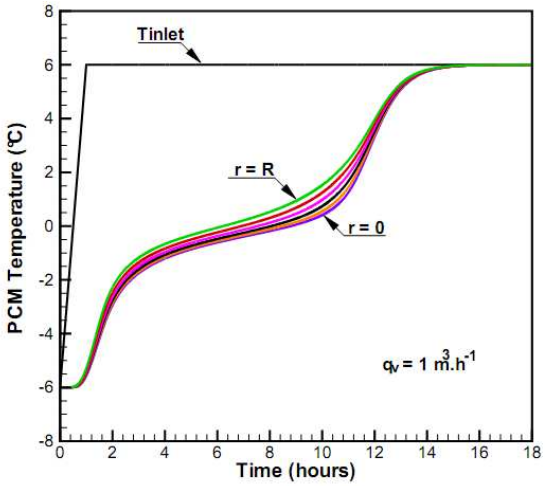

(c) Tank outlet

Fig.4: PCM temperature evolution within the capsules at different locations in the tank

In addition, the physical model permits to determine the evolution of the global liquid fraction of the PCM inside the tank, which allows identifying the end of the latent discharge process (see **Fig.5**). It should be noted that the liquid fraction varies between 0 and 1, when the PCM temperature is around its melting temperature T_m, e.g. within the temperature range of the phase transition $T_m - \frac{\Delta T}{2}$ and $T_m + \frac{\Delta T}{2}$. Below or above the temperature range, the value of the liquid fraction become 0 or 1, respectively. In general, the liquid fraction inside each capsule can be presented in the simulation by either straight line temperature-dependent discontinuous functions using conditional statements [63] or simplified temperature-dependent continuous functions [62]. However, a number of researchers [62-64] have noted that using discontinuous functions increases the computational time of simulation.

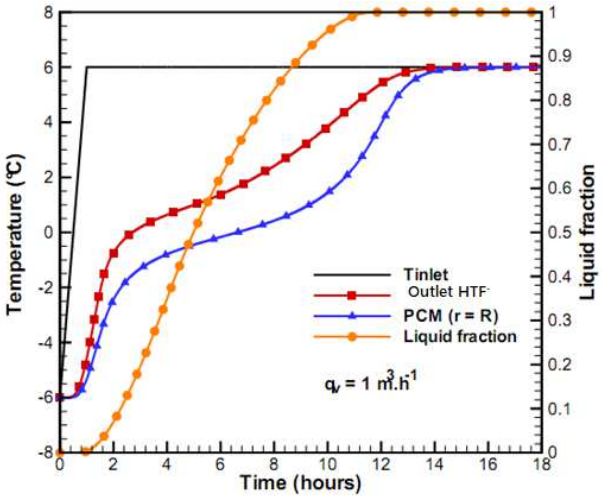

Fig.5: Global liquid fraction of the PCM versus time

The influence of the capsule diameter on the thermal performance of the tank was examined and presented in **Fig.6**. Three diameters were considered: d_{pcm} = 44 mm; d_{pcm} = 64 mm and d_{pcm} = 77 mm. We observe that as the capsule diameter decreases, the discharge time is reduced. Reducing the capsule diameter results in an increase in the number of capsules and consequently the area of exchange between the PCM capsules and the HTF. For the three diameters considered, all the latent thermal energy due to the melting has been recovered by the HTF.

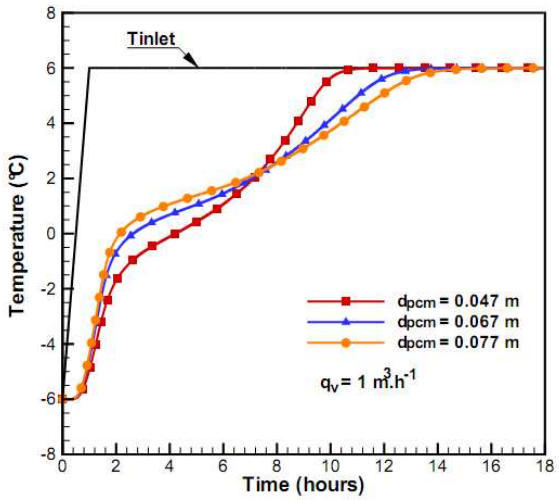

Fig.6: HTF temperature at the tank outlet versus time for various capsule diameter

The PCM temperature profile inside the capsules for the three diameters in the middle of the tank has been indicated in **Fig.7**. We note that for the same flow rate and at the same position in the tank, the thermal gradient within the capsules rises as the capsule diameter increases. These plots also confirm that the duration of the phase change within the capsules diminishes as the capsule diameter is reduced. In general, there is a compromise to be found between the HTF flow rate and the capsule diameter to improve heat transfer and minimize pumping power. Khattari et al. **[42]** demonstrated that for reasonably low values of HTF flow rate, the use of large size of spherical capsules can be advantageous for both thermal efficiency of the packed bed and pumping performance.

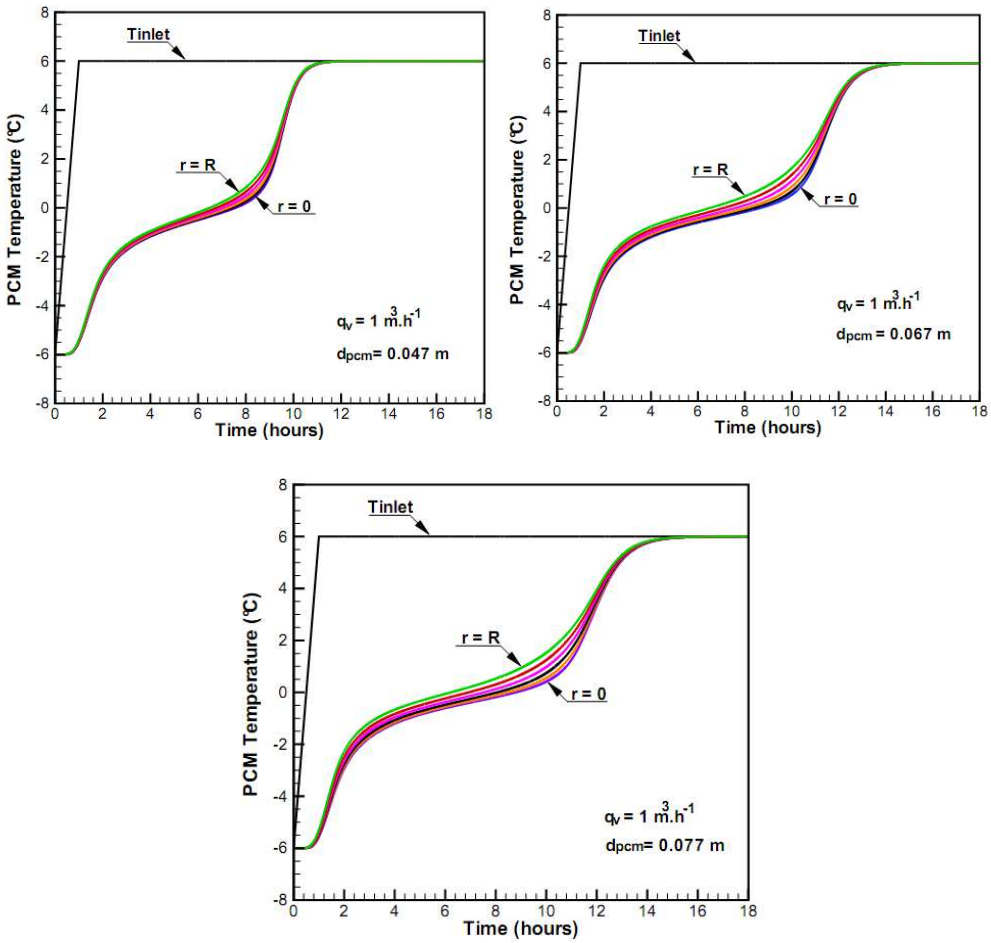

Fig.7: PCM temperature variation inside the capsule for various diameter

Fig.8 illustrates the impact of tank height on the discharge duration. We notice that the higher the height of the tank, the longer the discharge period, which appears to be coherent since an increase in height, induces an increase in the number of capsules, which implies to have an important quantity of PCM to melt inside the tank.

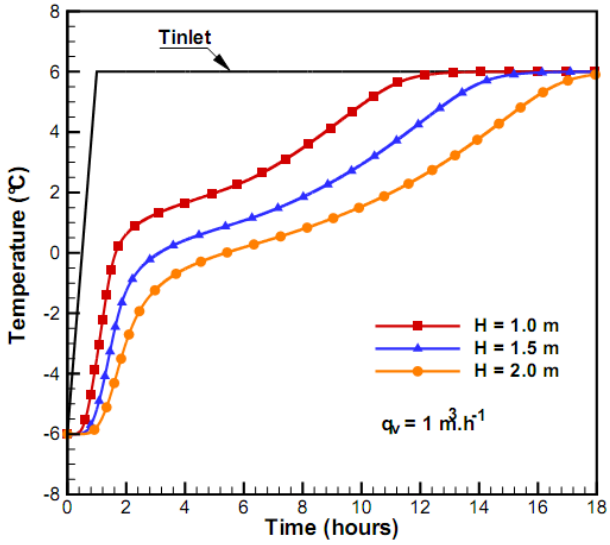

Fig.8: HTF temperature at the tank outlet versus time for various tank size

Fig.9 shows the evolution of the HTF temperature at the tank outlet for three initial temperatures (T_i = -8°C; -6°C; -4°C). The curves follow a completely similar pattern during the discharge. They differ only in the discharge time, which is slightly delayed as the initial temperature is raised. Therefore, the initial temperature does not have a great influence on the duration of the discharge process.

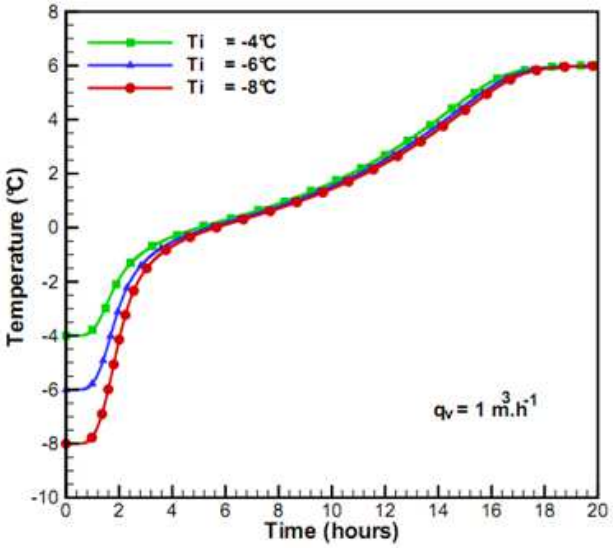

Fig.9: HTF temperature at the tank outlet versus time for various initial temperature

Conclusion

The physical model based on the apparent heat capacity method was implemented in this study. This model allowed us to analyse the phase transition inside the spherical capsules and to investigate the influence of different parameters on the thermal behaviour of the tank during the discharge period. It was also observed that the higher the height of the tank, the longer the discharge period. Increasing the diameter of capsules from 47 mm to 77 mm leads to increase the discharging period by about 30 %. In addition, varying the storage tank initial temperature between -8 °C to – 4 °C does not have a significant effect of on the discharging time.

From this investigation, we can conclude that:

- The system operation is strongly influenced by the size of the tank and the HTF flow rate.

- The reduction in capsule diameter reduces the discharge time. There is a compromise to be found between the HTF flow rate and the capsule diameter to improve heat transfer and minimize pumping power.
- The thermal performance of the system is slightly impacted by the initial conditions.

It is therefore important to dimension the storage tank according to the available power so that the discharge process is complete. The HTF flow rate will be chosen in order to recover the thermal energy stored within the required time.

Acknowledgments: This research was carried under the framework of E2S UPPA supported by the "Investissements d'Avenir" French programme managed by ANR (ANR-16-IDEX-0002)

References

[1] L. F. Cabeza, Advances in thermal energy storage systems: Methods and applications. Second Edition. Woodhead Publishing Series in Energy. Elsevier 2021.

[2] D. Li, J. Wang, Y. Ding, H. Yao, Y. Huang, Dynamic thermal management for industrial waste heat recovery based on phase change material thermal storage. Appl. Energy 236 (2019) 1168–1182.

[3] E. Oró, A. de Gracia, A. Castell, M.M. Farid, L.F. Cabeza, Review on phase change materials (PCMs) for cold thermal energy storage applications. Applied Energy 99 (2012) 513–533.

[4] M.A. B. Taher, H. El-Otmany, T. El Rhafiki, T. Kousksou, Y. Zeraouli, Inverse method to describe crystallization of undercooled water in cold storage tank. Journal of Energy Storage 36 (2021) 102404.

[5] M.A. Said, H. Hassan, Parametric study on the effect of using cold thermal storage energy of phase change material on the performance of air-conditioning unit, Appl.Energy 230 (2018) 1380–1402.

[6] B. Lamrani, T. Kousksou, Numerical investigation of a shell-and-tube latent heat thermal energy storage system for urban heating network. Journal of Energy Storage 43 (2021) 103216

[7] F. Bentivoglio, S. Rouge, O. Soriano, A. Tempass de Sousa, Design and operation of a 180 kWh PCM heat storage at the Flaubert substation of the Grenoble urban heating network, Appl. Therm. Eng. 185 (2021) 116402.

[8] Q. Ren, P. Guo, J. Zhu, Thermal management of electronic devices using pin-fin based cascade microencapsulated PCM/expanded graphite composite, Int. J. Heat Mass Tran. 149 (2020) 119199.

[9] B. Lamrani, B. E. Lebrouhi, Y. Khattari, T. Kousksou, A simplified thermal model for a lithium-ion battery pack with phase change material thermal management system. Journal of Energy Storage 44 (2021) 103377.

[10] M. Boulakhbar, B. Lebrouhi, T. Kousksou, S. Smouh, A. Jamil, M. Maaroufi, M. Zazi, Towards a large-scale integration of renewable energies in Morocco. Journal of Energy Storage 32 (2020) 101806.

[11] Y. Dong, F. Wang, Y. Zhang, X. Shi, A. Zhang, Y. Shuai, Experimental and numerical study on flow characteristic and thermal performance of macro- capsules phase change material with biomimetic oval structure, Energy 238 (2022), 121830.

[12] X. Cheng, X. Zhai, X. Wangc, P. Lina, Numerical study of forced convection over phase change material capsules in a traditional spherical shape and a biomimetic shape. Journal of Energy Storage 31 (2020) 101526

[13] C. Prietoa, L. F. Cabeza, Thermal energy storage (TES) with phase change materials (PCM) in solar power plants (CSP). Concept and plant performance. Applied Energy 254 (2019) 113646.

[14] M. Huang, W. He, A. Incecik, M. K. Gupta, G. Królczyk, Z. Li, Phase change material heat storage performance in the solar thermal storage structure employing experimental evaluation. Journal of Energy Storage 46 (2022) 103638.

[15] W. Liu, Y. Bie, T. Xu, A. Cichon, G. Królczyk, Z. Li, Heat transfer enhancement of latent heat thermal energy storage in solar heating system: A state-of-the-art review. Journal of Energy Storage 46 (2022) 103727.

[16] B. Sun, Z. Liu, X. Ji, L. Gao, D. Che, Thermal energy storage characteristics of packed bed encapsulating spherical capsules with composite phase change materials. Applied Thermal Engineering 201 (2022) 117659.

[17] V. Athawale, A. Bhattacharya, P. Rath, Prediction of melting characteristics of encapsulated phase change material energy storage systems. International Journal of Heat and Mass Transfer 181 (2021) 121872.

[18] Z. Liu, Z. Yu, T. Yang, D. Qin, S. Li, G. Zhang, F. Haghighat, M.M. Joybari, A review on macro-encapsulated phase change material for building envelope applications, Build. Environ. 144 (2018) 281–294.

[19] M. M. Kenisarin, K. Mahkamov, S. C. Costa, I. Makhkamova, Melting and solidification of PCMs inside a spherical capsule: A critical review. Journal of Energy Storage 27 (2020)101082.

[20] H.Asgharian E.Baniasadi, Experimental and numerical analyses of a cooling energy storage system using spherical capsules. Applied Thermal Engineering 149 (2019) 909-923.

[21] M. P.Vikram, V.Kumaresan, S.Christopher, R.Velraj, Experimental studies on solidification and subcooling characteristics of water-based phase change material (PCM) in a spherical encapsulation for cool thermal energy storage applications. International Journal of Refrigeration 100 (2019) 454-462.

[22] A.D. Gracia, L.F. Cabeza, Numerical simulation of a PCM packed bed system: a review, Renew. Sustain. Energy Rev. 69 (2017) 1055–1063.

[23] K. Nagano, S. Takeda, T. Mochida, K. Shimakura, Thermal characteristics of a direct heat exchange system between granules with phase change material and air, Appl. Therm. Eng. 24 (2004) 2131–2144.

[24] K.A.R. Ismail, R. Stuginsky Jr., A parametric study on possible fixed bed models for pcm and sensible heat storage, Appl. Therm. Eng. 19 (1999) 757–788.

[25] T.M. Sanderson, G.T. Cunningham, Performance and efficient design of packed bed thermal storage systems. Part 1, Appl. Energy 50 (1995) 119–132.

[26] A.F. Regin, S.C. Solanki, J.S. Saini, An analysis of a packed bed latent heat thermal energy storage system using PCM capsules: numerical investigation, Renewable Energy 34 (2009) 1765–1773.

[27] E. Tumilowicz, C.L. Chan, P. Li, B. Xu, An enthalpy formulation for thermocline with encapsulated PCM thermal storage and benchmark solution using the method of characteristics, Int. J. Heat Mass Transfer 79 (2014) 362–377.

[28] M. Cheralathan, R. Velraj, S. Renganarayanan, Heat transfer and parametric studies of an encapsulated phase change material based cool thermal energy storage system, J. Zhejiang Univ., SCIENCE A, 11 (2006) 1886–1895.

[29] A. Benmansour, M.A. Hamdan, A. Bengeuddach, Experimental and numerical investigation of solid particles thermal energy storage unit, Appl. Therm. Eng. 26 (2006) 513–518.

[30] C. Arkar, B. Vidrih, S. Medved, Efficiency of free cooling using latent heat storage integrated into the ventilation system of a low energy building, Int. J. Refrig. 30 (2007) 134–143.

[31] M. Rady, Thermal performance of packed bed thermal energy storage units using multiple granular phase change composites, Appl. Energy 86 (2009) 2704–2720.

[32] S. Wu, G. Fang,Dynamic performances of solar heat storage system with packed bed using myristic acid as phase change material, Energy Build. 43 (2011) 1091–1096.

[33] A. Raul, M. Jain, S. Gaikwad, S.K. Saha, Modelling and experimental study of latent heat thermal energy storage with encapsulated PCMs for solar thermal applications, Appl. Therm. Eng. 143 (2018) 415–428.

[34] K.A.R. Ismail, J.R. Henriquez, Numerical and experimental study of spherical capsules packed bed latent heat storage system, Appl. Therm. Eng. 22 (2002) 1705–1716.

[35] L. Yang, X. Zhang, G. Xu, Thermal performance of a solar storage packed bed using spherical capsules filled with PCM having different melting points, Energy Build. 68 (2014) 639–646.

[36] M. Wu, C. Xu, Y.L. He, Dynamic thermal performance analysis of a molten-salt packed-bed thermal energy storage system using PCM capsules, Appl. Energy 121 (2014) 184–195.

[37] P.A. Galione, C.D. Perez-Segarra, I. Rodríguez, O. Lehmkuhl, J. Rigola, A new thermocline-PCM thermal storage concept for CSP plants. Numerical analysis and perspectives, Energy Procedia 49 (2014) 790–799.

[38] H. Peng, H. Dong, X. Ling, Thermal investigation of PCM-based high temperature thermal energy storage in packed bed, Energy Convers. Manage. 81 (2014) 420–427.

[39] M. Wu, C. Xu, Y. He, Cyclic behaviors of the molten-salt packed-bed ther- mal storage system filled with cascaded phase change material capsules, Appl. Therm. Eng. 93 (2016) 1061–1073.

[40] A. Elouali, T. Kousksou, T. El Rhafiki, S. Hamdaoui, M. Mahdaoui, A. Allouhi, Y. Zeraouli,, Physical models for packed bed: Sensible heat storage systems. Journal of Energy Storage 23 (2019) 69-78

[41] E. Tumilowicz, C. L. Chan, P. Li, et B. Xu, An enthalpy formulation for thermocline with encapsulated PCM thermal storage and benchmark solution using the method of characteristics. Int. J. Heat Mass Transf., vol. 79 (2014) 362-377.

[42]Y.Khattari, E.H.Sebbar, Y.Chaibi, T.El.Rhafiki, T.Kousksou, Y.Zeraouli, Numerical study of a positive latent cold storage system for industrial applications: Discharge mode. Journal of Energy Storage 40 (2021)102824.

[43] T. Kousksou, P. Bruel, Encapsulated phase change material under cyclic pulsed heat load, Int. J. Refrig. 33 (2010) 1648–1656.

[44] J. O. Khor, L. Yang, B. Akhmetov, A. Bano Leal, A. Romagnoli, Application of granular materials for void space reduction within packed bed thermal energy storage system filled with macro-encapsulated phase change materials. Energy Conversion and Management 222 (2020) 113118

[45] B. Sun, Z. Liu, X. Ji, L. Gao, D. Che, Thermal energy storage characteristics of packed bed encapsulating spherical capsules with composite phase change materials. Applied Thermal Engineering 201 (2022) 117659.

[46] H. Peng, H. Dong, et X. Ling, Thermal investigation of PCM-based high temperature thermal energy storage in packed bed. Energy Convers. Manag. 81(2014) 420-427.

[47] M. A. Izquierdo-Barrientos, C. Sobrino, et J. A. Almendros-Ibáñez. Thermal energy storage in a fluidized bed of PCM », Chem. Eng. J. 230 (2013) 573-583.

[48] A. Tafone, E. Borri, L. F. Cabeza, A. Romagnoli, Innovative cryogenic Phase Change Material (PCM) based cold thermal energy storage for Liquid Air Energy Storage (LAES) – Numerical dynamic modelling and experimental study of a packed bed unit. Applied Energy 301 (2021) 117417.

[49] M-J. Li, B. Jina, Z. Maa, F. Yuan, Experimental and numerical study on the performance of a new high-temperature packed-bed thermal energy storage system with macroencapsulation of molten salt phase change material. Applied Energy 221 (2018) 1–15

[50] M-J. Li, B. Jin, J-J. Yan, Z. Ma, M-J. Li, Numerical and Experimental study on the performance of a new two-layered high-temperature packed-bed thermal energy storage system with changed-diameter macro-encapsulation capsule. Applied Thermal Engineering 142 (2018) 830–845.

[51] J. Beek, Design of packed catalytic reactors, Adv. Chem. Eng. (1962) 203–271.

[52] A. Halimov, M. Lauster, D. Müller, alidation and integration of a latent heat storage model into building envelopes of a high-order building model for Modelica library AixLib. Energy & Buildings 202 (2019) 109336.

[53] J.M. Khodadadi, Y. Zhang, Effects of buoyancy-driven convection on melting within spherical containers, Int. J. Heat Mass Transf. 44 (8) (2001 Apr 1) 1605–1618.

[54] M. M. Kenisarin, K. Mahkamov, S. C. Costa, I. Makhkamova, Melting and solidification of PCMs inside a spherical capsule: A critical review. Journal of Energy Storage 27 (2020) 101082

[55] A. S. Soliman, S. Zhu, L. Xu, J. Dong, P. Cheng, Numerical simulation and experimental verification of constrained melting of phase change material in cylindrical enclosure subjected to a constant heat flux. Journal of Energy Storage 35 (2021) 102312.

[56] M. Lacroix, Numerical simulation of a shell-and-tube latent heat thermal energy storage unit, Sol. Energy. 50 (1993) 357–367.

[57] S. Patankar, Numerical heat transfer and fluid flow, Taylor & Francis, 2018.

[58] J.P. Bédécarrats, J. Castaing-Lasvignottes, F. Strub, J.P. Dumas, Study of a phase change energy storage using spherical capsules. Part I: Experimental results. Energy Conversion and Management 50 (2009) 2527–2536.

[59] J.P. Bédécarrats, F. Strub, B. Falcon, J.P. Dumas, Phase-change thermal energy storage using spherical capsules: performance of a test plant. Int. J. Refrigeration 19 (1996) 187-196

[60] T. Kousksou, J. Bedecarrats, J.P. Dumas, A. Mimet, Dynamic modelling of the storage of an encapsulated ice tank. Applied Thermal Engineering 25 (2005) 1534-1548.

[61] P.H. Biwole, D. Groulx, F. Souayfane, T. Chiu, Influence of fin size and distribution on solid-liquid phase change in a rectangular enclosure, Int. J. Thermal Sci. 124 (2018) 433–446.

[62] Y. Khattari, H. El-Otmany, T. El Rhafiki, T. Kousksou, A. Ahmed, E. Ben Ghoulam, Physical models to evaluate the performance of impure phase change material dispersed in building materials. Journal of Energy Storage 31 (2020) 101661.

[63] I. Medved, A. Trník, L. Vozár, Modeling of heat capacity peaks and enthalpy jumps of phase-change materials used for thermal energy storage. International Journal of Heat and Mass Transfer 107 (2017) 123–132.

[64] F. Jorissen, M. Wetter, L. Helsen, Simulation speed analysis and improvements of modelica models for building energy simulation, in: Proceeding of the 11th International Modelica Conference, LBNL-1002904, 2015, pp. 57–69,